Analysis of void formation in thermoplastic composites during resistance welding

Huajie Shi*, Irene Fernandez Villegas, Harald E.N. Bersee

Structural Integrity and Composites, Faculty of Aerospace Engineering, Delft University of Technology, Kluyverweg 1, 2629 HS Delft, the Netherlands

Abstract

The process induced voids during resistance welding of glass fabric reinforced polyetherimide was investigated. The mechanisms of void formation in adherends, in particular the residual volatile induced voids and the fibre de-compaction induced voids, were analyzed. Due to the non-uniform temperature and stress distributions in the joints during welding, a non-uniform void distribution was observed in the joints, with more voids generated in the middle of the joints than at the edges. Welding temperature and pressure were shown to have a large influence on void formation. Increasing of welding pressure was shown to effectively reduce the voids, while the residual moisture induced voids were found more difficult to be eliminated than the fibre de-compaction induced voids.

Keywords

Thermoplastic, composites, resistance welding, voids, polyetherimide

Introduction

By locally melting and consolidating thermoplastics at the interface, welding has been found to be a fast and cost effective joining method for thermoplastic composites. Among the various welding techniques, resistance welding is one of the most interesting and mature techniques. [1-4] Being a thermal process, the quality of resistance welded joints is highly dependent on the welding parameters, [4,5] i.e. welding pressure, power input

and heating time. A deeper review of the welding process, including heat generation, heat transfer and crystallization kinetics, is given by Maffezzoli, A. M., et al.[6] Voids, or porosities, have been found to be an issue in thermal processing of thermoplastic composites,[5, 7-9] during which re-heating of composites is a necessary procedure. Voids are sometimes observed in the weld line or in the adherends of resistance welded thermoplastic composite joints.[5, 10-12] The presence of voids is shown to have an influence on the mechanical performance of the joints.[5,13,14] Therefore, understanding the mechanisms of void formation in resistance welding of thermoplastic composites is important for improving the welding process.

Resin impregnation and void reduction are key steps for manufacturing of thermoplastic composites using processes such as liquid matrix impregnation,[15,16] tow-placement[17, 18] and impregnation of commingled thermoplastic composite yarns.[19, 20] The origin of interbundle and intrabundle voids is related to interbundle flow and intrabundle flow, respectively, and a study of two-scale impregnation is performed by Gennaro, R., et al.[19] Welding of thermoplastic composites, however, is secondary processing of fully consolidated laminates, and there are no initial interbundle or intraply voids before welding. In literatures, many hypotheses have been proposed aiming to explain void generation during welding of thermoplastic composites.[5,8,10,12,21-24] Voids were observed in the weld line of dual-polymer welded graphite-polyarylsulfone/polysulfone (PAS/PS) composites owing to trapped volatiles and overheating at the weld interface.[8] Xiao et al.[8] developed a thermal buckling model to analyze voids and de-consolidation induced during induction heating of carbon fibre reinforced polyetheretherketone (CF/PEEK), and indicated that thermal stress induced in the non-uniform temperature fields of the parts was the cause of voids. Ageorges et al.[5] attributed voids generated in resistance welding of carbon fibre reinforced polyetherimide (CF/PEI) to the de-consolidation of laminates subjected to an inadequate welding pressure, e.g. lower than 0.2 MPa. A similar explanation was also used for void generation during resistance welding of metal-thermoplastic composites[25]

and thermosetting composites-thermoplastic composites.[21] Ye et al.[23,24]proposed a “void growth, migration and closure” model for thermal processing of thermoplastic composites where de-consolidation and re-consolidation were regarded as the main driving forces for void growth, migration and closure. More recently, Dubé et al.[12] attributed the process induced voids in resistance welding of glass fibre reinforced polyetherimide (GF/PEI) and CF/PEI to two phenomena: (1) a reduction of pressure in the joints caused by the squeezing out of the polymer; (2) the relatively low environmental resistance of the PEI polymer. Despite all these studies, a comprehensive understanding of the mechanisms involved in void formation and void distribution in resistance welding of thermoplastic composites considering the inherent non-uniform temperature distribution in the joints, is still missing.

In this study, both a theoretical analysis and an experimental investigation were performed to better understand void formation in adherends during resistance welding of GF/PEI composites. In order to narrow down the possible causes of void formation to investigate in this study, preliminary thermomechanical analysis (TMA) tests were performed on ambient conditioned neat PEI specimens (with residual moisture) and GF/PEI composites specimens (without residual volatiles). Voids were found in both specimens after a thermal cycle with a plateau temperature of 300 °C (the glass transition temperature of PEI is 215 °C[26]). Since there was no resin flow or severe temperature gradients in the specimens, the voids cannot be caused by resin squeeze flow or thermal buckling. Residual moisture and fibre de-compaction were thought to be the most likely causes of voids in these PEI and GF/PEI specimens, respectively. Therefore, the focus of this study was set on voids induced by residual volatiles and fibre de-compaction.

Experimental

Materials

The adherends used for welding were made of eight layers of 8HS woven GF/PEI prepregs, supplied by TenCate, the Netherlands. The GF/PEI laminates, with a stacking sequence of $[(0/90)]_{4S}$, were consolidated in a hot platen press at a processing temperature of 320 °C and a consolidation pressure of 2.0 MPa for 20 minutes. The obtained laminates had a resin volume fraction of around 50%. Adherend plates of 192 mm × 50 mm were cut from the large laminates using a water-cooled diamond saw. A plain woven metal mesh made of AISI 304L stainless steel, with a wire diameter of 0.04 mm and gap of 0.09 mm, was used as the heating element. Mesh strips of 250 mm × 13 mm were cut from larger sheets of metal mesh and used as the heating elements for the resistance welding. To provide a resin rich area at the welding interface, the mesh was sandwiched between two layers of 60 µm thick PEI resin films prior to the welding process.

Welding process

An in-house developed resistance welding setup,[14] was used to weld the joints. The welding energy was provided by a computer controlled power supply unit, with a maximum DC output of 45 A and 70 V, from Delta Elektronika. The resistance welding process was controlled by a labview program. The welding parameters, i.e. current, voltage and temperature, were recorded during the welding process using a data acquisition (DAQ) system. The clamping pressure and welding pressure were applied using two separate pneumatic systems. High-density fibre wood blocks were used as the thermal insulators. Predefined appropriate welding parameters, i.e. 80 kW/m^2 for the power input and 55 s for the heating time,[14] were used to weld all the joints.

Measurement of void content

The void distributions of the joints were inspected using Zeiss Axiovert 40 MAT optical microscope at a magnification of 2.5×. The middle parts of the joints were used to rule out possible "edge effects", such as too high or too low temperatures near the edges. The specimens were cut off, embedded in an epoxy resin (Tecnovit® 4071), polished and observed. Grey-scale images were captured for the cross-sections of the joints, and then these images were used for quantitative analysis. The void content of the cross-sections was calculated using digital image processing procedures, including image trimming, image filtering, image binaryzation and pixel statistics.

Measurement of residual volatiles

When exposed to an open environment, PEI tends to absorb moisture from the surroundings until it reaches a saturation state. Additionally, residual N-methyl-2-pyrrolidone (NMP), a solvent used in fabrication of GF/PEI prepreg, is usually present in the GF/PEI pregregs as received. The boiling temperature of NMP in atmosphere is 204.3 °C.[27] The contents of residual moisture and NMP in the GF/PEI composites were measured using drying tests. To measure the weight fraction of residual NMP in GF/PEI, the prepreg was put in an oven at 135 °C for 12 h to prevent the possible influence of residual moisture, and then it was dried at 260 °C for 3 h. The fraction of residual NMP was calculated by weighing the prepreg before and after the final drying process. Since GF/PEI laminates can also absorb moisture from their surroundings after fabrication, the weight fraction of residual moisture in the laminates was measured in a similar way: drying the laminates in an oven at 135 °C until a steady weight was achieved, and measuring the weight before and after the final drying process.

Analysis

Thermal and stress analysis

As a typical non-isothermal process, resistance welding of thermoplastic composites usually results in non-uniform temperature distributions in the joints both along the weld line and in the through-the-thickness direction.[28] As the stiffness of a thermoplastic matrix is highly dependent on the welding temperature, the distribution of welding pressure (or internal stress) in the joints could also be non-uniform, which in turn would influence void generation and void distribution inside the joints. Therefore, to analysis the void formation and distribution in resistance welding, the thermal behaviour and stress distributions of the joints should be determined first.

A 2D heat transfer model, as shown in Figure 1 (a), was developed using COMSOL Multiphysics® 4.3b to simulate the temperature distribution of joints in resistance welding. The welding energy was provided by Joule heating of the metal mesh heating element. The governing equation of heat transfer is:

$$\rho C_p \frac{\partial T}{\partial t} = \dot{q} + k_{xx}\frac{\partial^2 T}{\partial x^2} + 2k_{xy}\frac{\partial^2 T}{\partial x \partial y} + k_{yy}\frac{\partial^2 T}{\partial y^2} \quad (1)$$

where ρ is the density, C_p is the heat capacity, $\dot{q}$ is the heat generation rate from the heating element and k is the thermal conductivity.

The relevant material properties are listed in Table 1. Temperature dependent material properties were used for GF/PEI laminates and PEI film, as listed in Table 2. The material properties for the PEI resin were provided by the supplier, and the temperature dependent specific heat of GF/PEI was measured using differential scanning calorimetry (DSC) tests according to ASTME1269-11. The temperature dependent thermal conductivity of GF/PEI laminates was measured in the laboratories of the Koninklijke DSM N.V., the Netherlands using the laser flash method.

Table 1. Material properties at room temperature for heat transfer model

Material properties	Density ρ (kg/m^3)	Specific heat C_p (J/kg·°C)	Thermal conductivity k_{xx}, k_{yy} (W/m·°C)	k_{zz} (W/m·°C)	Reference
Metal mesh	7780	460	10	10	Ref 28
Wood insulator	1242	1090	0.12	0.12	Ref 28
PEI resin film	1270	980	0.22	0.22	ρ, k: Ref 26; C_p: Ref 29
GF/PEI	1930	890	0.53	0.4	Measured

Table 2. Temperature dependent material properties of GF/PEI and PEI

Temperature (°C)	GF/PEI Specific heat (Measured) C_p (J/kg·°C)	GF/PEI Thermal conductivity (Measured) k_{xx}, k_{yy} (W/m·°C)	GF/PEI Thermal conductivity (Measured) k_{zz} (W/m·°C)	PEI Specific heat[28] C_p (J/kg·°C)	PEI Thermal conductivity[28] k (W/m·°C)
20	890	0.53	0.4	980	0.22
70	1000	0.57	0.43	1180	0.23
120	1090	0.59	0.44	1360	0.24
170	1150	0.6	0.45	1518	0.25
220	1340	0.65	0.49	1865	0.26
270	1450	0.68	0.38	1963	0.26

The boundaries of the heat transfer model were set to be free convection with surface-ambient radiation, as described in:

$$-n \cdot (-k\nabla T) = h(T_{amb} - T) + \varepsilon\sigma(T_{amb}^4 - T^4) \quad (2)$$

where the free convection coefficient $h = 5\mathrm{W/m^2 \cdot K}$,[30] the ambient temperature $T_{amb} = 20°C$, surface emissivity $\varepsilon = 0.95$[30] and the Stefan-Boltzmann constant $\sigma = 5.67 \times 10^{-8} W/m^2K^4$.

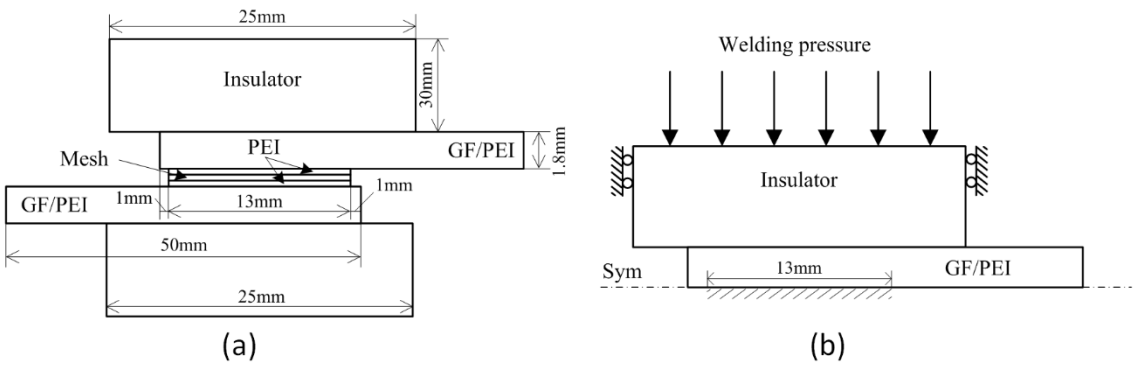

Figure 1. The geometry and boundary conditions of resistance welding for (a) heat transfer analysis, and (b) inner stress analysis.

Stress analysis was performed also in COMSOL Multiphysics® 4.3b, and the heat transfer model was coupled with the structural analysis model to predict the inner stresses of the joints during welding. Several assumptions were made in the structural analysis model: (1) the inner stress was analysed using a cross-section 2D plane strain model by assuming that the length of the joints (192 mm) is much higher than the overlap width (12.7 mm) and there is no strain along the longitudinal direction; (2) due to much smaller thickness thinness of the metal mesh heating element as compared to the composites, the weld line was not considered in the model; (3) due to the symmetry in geometry, only half of the model was used for the stress analysis; (4) thermal expansion was not considered in the model, because the effect of thermal expansion

should be much smaller than the effect of modulus change with temperature increasing during welding, so this should not have a significant impact in the results. The geometry and boundary conditions of the model are illustrated in Figure 1(b), where the weld overlap area is defined as a fixed wall and a constant welding pressure uniformly applied to the top of the insulator. The mesh consists of triangular elements with quadratic shape functions, and the total number of element is 2124. The relevant material properties at room temperature are listed in Table 3.

Table 3. Material properties at room temperature for stress analysis

Material	Young's Modulus - E (GPa)	Poisson's ratio - ν
Wood insulator	12.4[31]	0.3[31]
Glass fibre	73[32]	0.22[32]
PEI	4.63 (Measured by DMA)	0.36[26]
GF/PEI	8.71* (Predicted using rules of mixture)	0.3 (Assumption)

* Out-of-plane Modulus

Since mostly compressive loads are applied during the welding process, compressive stress should be the dominating stress in the joints. To simplify the problem, the GF/PEI laminate was assumed to be isotropic and a temperature dependent out-of-plane modulus was used. The temperature dependent out-of-plane modulus of GF/PEI, E_c, was approximately predicted from the modulus of fibre and polymer using the rule of mixtures[33]:

$$E_c = \frac{E_f \cdot E_m}{E_m V_f + E_f (1 - V_f)} \tag{3}$$

where E_f is the modulus of the fibre and E_m is the modulus of the matrix. E_f was assumed to be constant during the welding process, while the temperature dependent E_m was measured using dynamic mechanical analysis (DMA) and rheology. The DMA tests were performed from T_{room} to 240 °C with a heating rate of 2.5 °C/min

using a frequency sweep of 0.1 Hz ~ 100 Hz. As the shear rate of the matrix was believed to be low in resistance welding, the results measured with a frequency of 0.1Hz were used. For high temperature (T > 240 °C), rheology measurements were performed and E' (tensile storage modulus) was calculated from G' (shear storage modulus) using an assumed constant Poisson's ratio of 0.3. The calculated GF/PEI modulus are listed in Table 4.

Table 4. Temperature dependent modulus of GF/PEI in the through-thickness direction

Temperature - T (°C)	Storage Modulus of PEI - E' (GPa)	Storage Modulus of GF/PEI - E_c' (GPa)
20	4.63	8.71
50	4.26	8.43
100	4.17	7.88
200	3.7	7.03
237	0.07	0.14
270	3.16E-4*	6.32E-4
290	1.78E-4*	3.56E-4
300	1.18E-4*	2.36E-4
310	7.3E-5*	1.46E-4
320	4.3E-5*	8.60E-5

* Calculated using G', with an assumed Poisson's ratio of 0.3

Void formation due to fibre de-compaction

Since normally a relatively high consolidation pressure, 2.0 MPa for this study, is used for fabrication of thermoplastic composites, residual compression stresses could be stored in the consolidated laminates, especially for glass mat or woven fabric reinforced composites.[34-36] If the consolidated laminates are re-heated, the residual compression stress previously stored in the fabric might be released due to the reduction

of matrix stiffness at elevated temperatures. Such process is usually referred to as fibre de-compaction.[23] Several studies have been performed on the fibre de-compaction induced voids,[7,37] and in these studies a representative volume element (RVE) analysis is used by assuming a homogeneous composite material and resin flow through the fibre preform obeying Darcy's law. However, the voids generated during fibre de-compaction of GF/PEI were mainly concentrated in the resin rich area (see Figure 2), but not inside the yarns, so applying these assumptions in our material system could be questionable. In the present study, a simple analysis based on the mechanical equilibrium of the compressed fibre, as illustrated in Figure 2, was used to describe the process of fibre de-compaction. The detailed analysis is described in what follows.

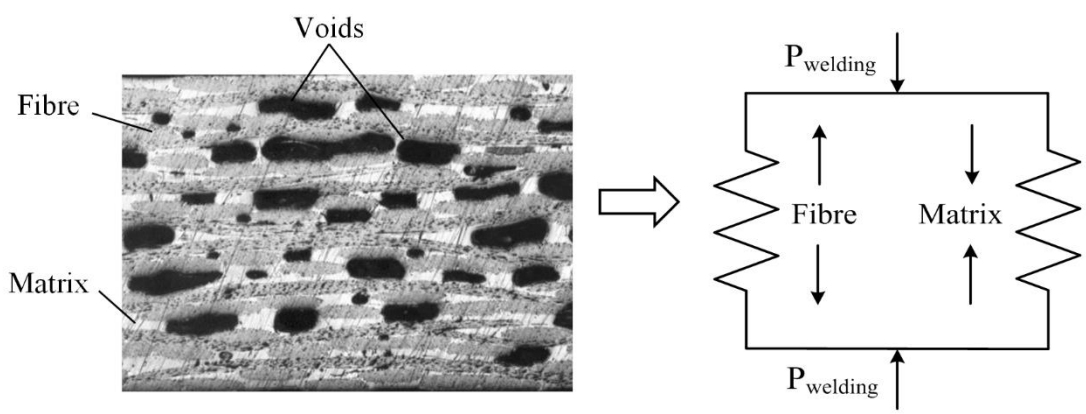

Figure 2. Mechanical equilibrium of the compressed fibre in a composite.

Initially, the fabric is constrained by the surrounding matrix and the applied welding pressure, where the applied welding pressure is assumed to mainly result in internal stresses in the matrix. The mechanical equilibrium can be expressed as follows:

$$\sigma_{f0} < \mathrm{UTS}_{\mathrm{matrix}}(\mathrm{T}) + \mathrm{P}_{\mathrm{welding}} \tag{4}$$

where σ_{f0} is the initial compressive stress of fabric in the consolidated laminate, $UTS_{matrix}(T)$ is the ultimate tensile strength of matrix at temperature-T, and $P_{welding}$ is the welding pressure applied on the laminates. The upper bound of $UTS_{matrix}(T)$ can be approximately calculated by

$$\mathrm{UTS_{matrix}(T) = E_{matrix}(T) \cdot e} \tag{5}$$

where $E_{matrix}(T)$ is the modulus of matrix at temperature T, and e is elongation of matrix at yield, i.e. $e = 0.07$ for PEI.[26] Since $E_{matrix}(T)$ decreases with increasing temperature, so does $UTS_{matrix}(T)$. Once $UTS_{matrix}(T)$ drops below σ_{f0}, the fabric could either be de-compacted or be further compressed, depending on the value of $P_{welding}$. Fibre de-compaction will happen when σ_{f0} becomes bigger than a critical stress, $\sigma_{critical}$, as expressed below:

$$\mathrm{\sigma_{f0} > \sigma_{critical} = UTS_{matrix}(T) + P_{welding}} \tag{6}$$

As fibre de-compaction progresses, the laminate thickness, H, will increase, and the fibre volume fraction, V_f, will decrease:

$$H_0 V_{f0} = H V_f \tag{7}$$

$$(H - H_0)/\mathrm{H} = V_v \tag{8}$$

where H_0 is the initial thickness of the laminate, V_{f0} is the initial volume fraction of the fibre, and V_v is the volume fraction of the voids. With decreasing fibre volume fraction, the residual compressive stress of the fabric will continually release until a new equilibrium is reached:

$$\sigma_f = UTS_{matrix}(T) + P_{welding} \approx P_{welding} \tag{9}$$

where σ_f is the residual compressive stress of the fabric, and it can be expressed by a power law function of fibre volume fraction, V_f.[7,38,39] With increasing laminate thickness, voids will fill the incremental volume of the laminate, as shown in Figure 2. As a result, the matrix will become disconnected, especially through the

thickness of the laminate, and therefore $UTS_{matrix}(T)$ will be reached. By ignoring $UTS_{matrix}(T)$ in the analysis, the final residual stress of the fabric, σ_f, should be approximately equal to the external pressure, $P_{welding}$. This means that the final de-compaction state should be mainly determined by the applied external pressure and the compressive properties of the fabric, which agrees with the results reported in literature.[37]

Void formation due to residual volatiles

The formation of volatile induced voids can be expressed using classical nucleation theory.[40-42] The distribution of residual volatiles inside the laminates is assumed to be uniform, and homogenous nucleation was used for the analysis. The effect of fibre on void nucleation is unknown, so it is neglected to simplify the problem. The formation of voids is a process of phase change, from liquid phase to gas phase, which requires excess energy to make up for the difference between the free energies of the two phases. Taking into account the changes of free volume and interfacial energies, the excess energy ΔG is equal to:[40,41]

$$\Delta G = 4\pi R^2\gamma - \frac{4}{3}\pi R^3(P_v - P_p) \tag{10}$$

where R is the radius of the void, γ is the surface tension of polymer-void interface, P_v is the pressure inside the void and P_p is the pressure of the surrounding polymer as a result of the welding pressure.

The critical radius of the void R_v^* (the radius corresponding to chemical equilibrium between the void and the surrounding polymer) and the minimum Gibbs free energy for nucleation of a critical nucleus ΔG^* are given by:[40]

$$R_v^* = 2\gamma/(P_v - P_p) \tag{11}$$

$$\Delta G^* = 16\pi\gamma^3/3(P_v - P_p)^2 \tag{12}$$

The critical void radius varies with the vapour pressure and the polymer pressure. The void nucleation rate J can be expressed by:[41,42]

$$J = N\sqrt{2\gamma/\pi m} \cdot exp(-16\pi\gamma^3/3k_bT(P_v - P_p)^2) \tag{13}$$

where N is the number of molecules per unit volume of the volatile phase, m is the mass of a gas molecule, k_b is the Boltzmann constant, 1.38×10^{-23}, and T is the absolute temperature. As void nucleation in the polymer can be assumed to occur instantaneously[43] and the rate of nucleation is proportional to the equilibrium number of critical size voids,[42] the probability of void nucleation can be calculated using the nucleation rate for any given spatial location and heating history.

After nucleation, the growth of voids in polymer can be assumed to be an idea spherical bubble growing in a Newtonian fluid[17,44], and RVE analysis can be used. The governing equation for void growth is given by:[17]

$$4\mu\left(\frac{R^3}{S^3} - 1\right)\frac{dR}{dt} + \left(P_v - P_p\right)R - 2\gamma = 0 \tag{14}$$

Where μ is the viscosity of the polymer, R is the radius of the void and S is the radius of the polymer shell. The polymer is assumed to be incompressible, and then the mass conservation of polymer yields:

$$S^3 - R^3 = {S_0}^3 - {R_0}^3 \tag{15}$$

According to the idea gas law, P_v can be calculated by the equation:

$$P_v = \frac{TP_{v0}R_0^3}{T_0R^3} \tag{16}$$

Substituting equations (14) and (15) into equation (13) yields:

$$4\mu\left(\frac{R_0^3 - {S_0}^3}{{S_0}^3 + R^3 - {R_0}^3}\right)\frac{dR}{dt} + \left(\frac{TP_{v0}R_0^3}{T_0R^3} - P_p\right)R - 2\gamma = 0 \tag{17}$$

Using this governing equation, the volume change of voids can be calculated.

Results and discussion

Temperature and stress distributions

The temperature distribution of GF/PEI joints during resistance welding was simulated and shown in Figure 3(a). Due to heat dissipation from the metal mesh to the surroundings, temperature gradients were observed in the though-the-thickness direction and along the weld overlap. The highest temperatures were found near the weld overlap, and similar temperature distributions are also found in literature.[28,45]

Due to the non-uniform temperature distribution, the welding pressure will be re-distributed inside the joints. Figure 3(b) shows the stress distributions of GF/PEI joints under a welding pressure of 0.8 MPa. Non-uniform stress distributions were observed, with stress concentrations near the edges of the weld overlap. The much lower internal stress in the middle of the joints relative to the edges was caused by the dramatic drop of the modulus of PEI resulting from the much higher welding temperature. The non-smooth stress gradient in the joints was caused by the non-continuity of the modulus of laminates subjected to the temperature gradient (the modulus of PEI changes several orders of magnitudes from room temperature to melting temperature).

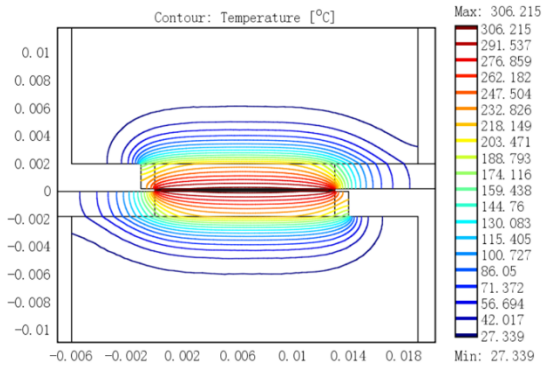

(a)

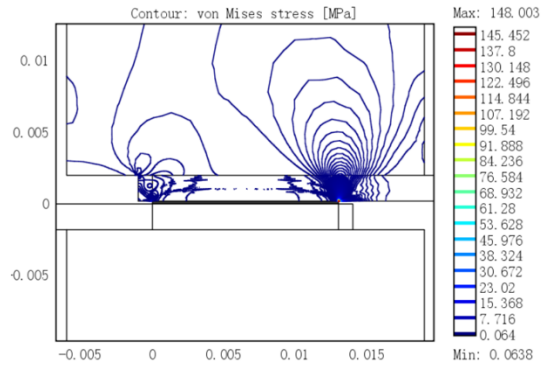

(b)

Figure 3. (a) The temperature distributions, and (b) stress distributions for resistance welding of GF/PEI, at a heating time of 55s.

Fibre de-compaction induced voids

The compressibility of glass fabric used in the laminates was characterized by a compression test. Eight layers of 7781 glass fabric 50 mm × 50 mm were stacked and compressed in a Zwick 20KN machine using a constant cross head speed of 0.05 mm/min. The thickness of the fabric assembly, H, can be converted into fibre volume fraction, V_f, by the equation:[34,36]

$$V_f = \frac{N_f \rho_a}{\rho_f H} \tag{18}$$

where N_f is the number of the fabric assembly been compressed, ρ_a is the surface density of the fabric and ρ_f is the density of glass fibre. In this study, $N_f = 8$, $\rho_a = 0.3\mathrm{kg/m^2}$ and $\rho_f = 2550\mathrm{kg/m^3}$.[31,46] A relationship between the compression force and the thickness of fabric assembly, H, was recorded by the machine. Based on that, a relationship between the fibre volume fraction, V_f, and the applied pressure, P, was calculated and fitted using a power law equation (see Figure 4). Having an average thickness of 1.78 mm for the GF/PEI laminates used in this study, the initial fibre volume fraction of the laminates was calculated to be 53% (using Eq.18), and then the initial compression pressure of the fabric was found to be 0.08 MPa according to Figure 4. It means that fibre de-compaction could only happen when the external pressure applied on the fabric was smaller than 0.08 MPa. Assuming the modulus of glass fibre remains constant during welding, the effect of temperature on the compression pressure of fabric was neglected in this analysis.

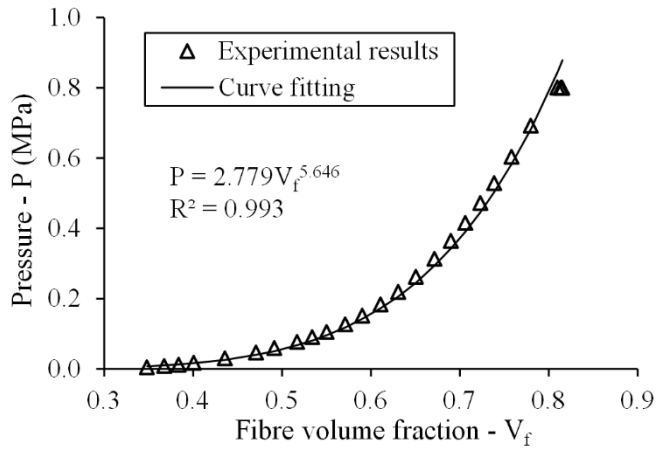

Figure 4. Compressibility of eight layers assembly of 7781 glass fabric.

Due to the non-uniform temperature distribution inside the joints, the distribution of $UTS_{matrix}(T)$ is also non-uniform. As the welding pressure, $P_{welding}$, will be re-distributed inside the joints during welding, the critical stress for fibre de-compaction, $\sigma_{critical} = UTS_{matrix}(T) + P_{welding}$ (see Eq.6), could vary a lot inside the joints. The distributions of $(UTS_{matrix}(T) + P_{welding})$ for the joints welded under different welding pressures of 0.1 MPa, 0.2 MPa, 0.4 MPa and 0.8 MPa and at the highest welding temperature (at a heating time of 55 s) are shown in Figure 5. The values of critical stresses were found to be higher near the middle of the weld overlap than the edges. It is related to the non-uniform temperature distribution in the joints: with higher welding temperatures in the middle of the joints than at the edges.[28] Relative big oscillations were found in the stress curves, which were probably induced by the big changes of modulus inside the joints as a result of the big temperature gradients. Having a much lower critical stress in the middle of the weld overlap, fibre de-compaction tends to happen more easily, and consequently more voids can be generated in the middle part of the joints. Using the initial compressive stress of fabric, 0.08 MPa, as the benchmark value, the

minimum welding pressure that was required to prevent the fibre de-compaction induced voids was found to be around 0.4 MPa.

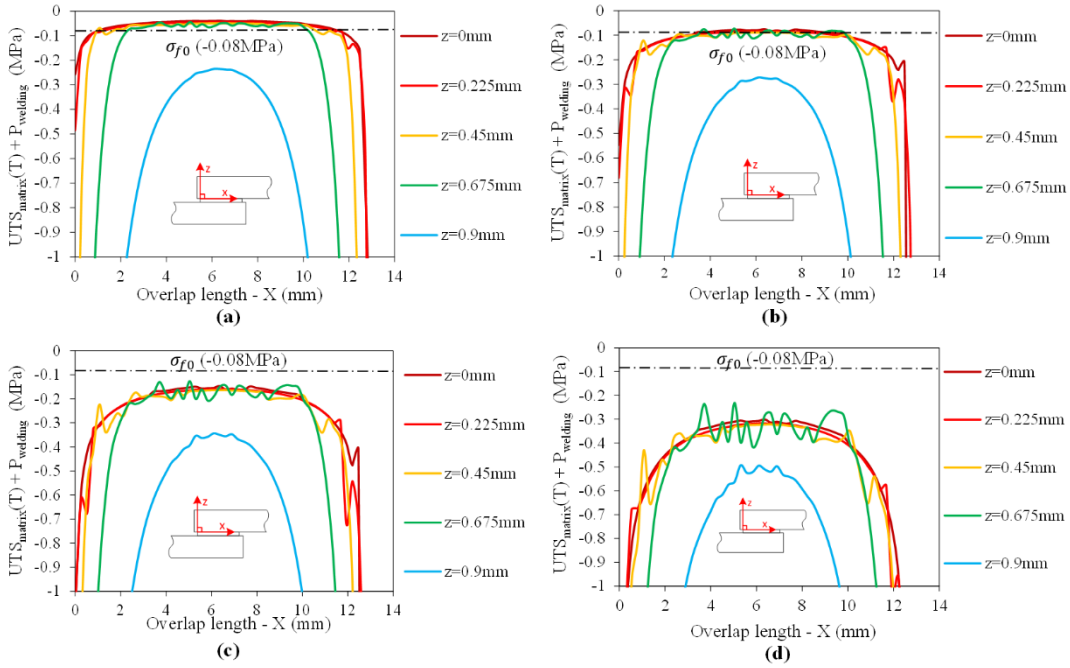

Figure 5. Distributions of critical stress for the GF/PEI joints welded with different pressures of 0.1 MPa, 0.2 MPa, 0.4 MPa and 0.8 MPa (the negative sign in the plots indicates a compressive stress).

An experimental study of fibre de-compaction induced voids in resistance welding of GF/PEI was performed. In order to prevent the possible influence of residual volatiles, the GF/PEI prepreg was dried in an oven at 260 °C for 3 hours before consolidation. After consolidation, the laminates were immediately welded or stored in desiccator before welding. The GF/PEI joints were welded at four different welding pressures of 0.1 MPa, 0.2 MPa, 0.4 MPa and 0.8 MPa. The cross-section microscopy images of the joints and the void distributions along the welding overlaps are plotted in Figure 6. Non-uniform void distributions were

observed inside the joints, with more voids concentrated near the middle part of the joints than the edges, showing agreement with the model prediction. Void content was found to decrease with increasing welding pressure. A considerable void content, i.e. higher than 1%, was obtained for the joints welded using a welding pressure of 0.2 MPa or 0.1 MPa, while a relatively small void content, less than 0.1%, was obtained for the joints welded with a welding pressure higher than 0.4 MPa. A welding pressure of around 0.4 MPa was found to be the critical welding pressure for preventing fibre de-compaction induced voids, in accordance with the model prediction.

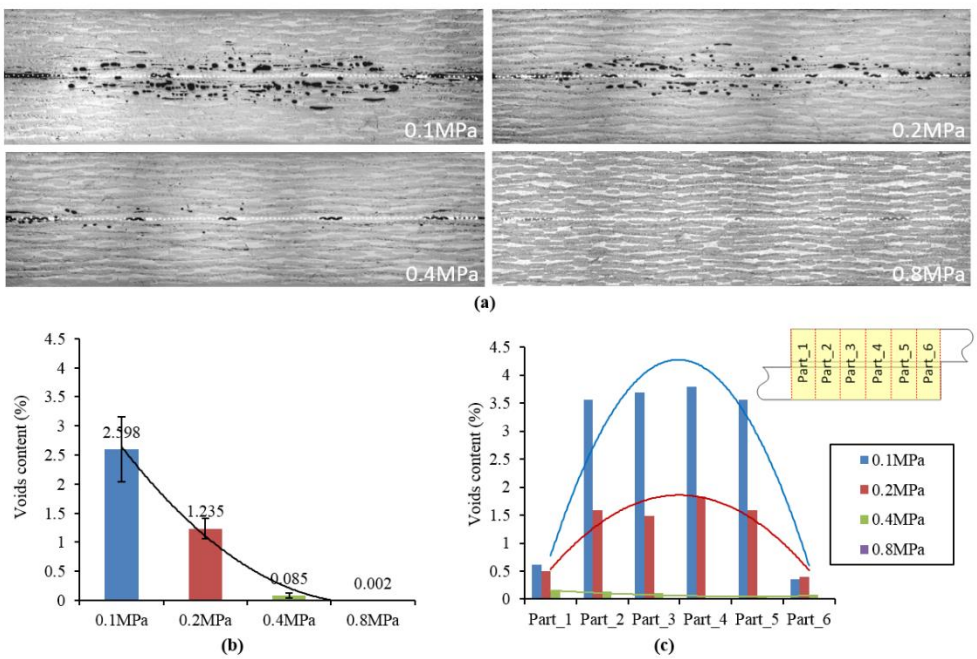

Figure 6. (a) Cross-section micrographs, (b) average void contents and (c) void distributions along the weld overlap of GF/PEI joints welded with different pressure of 0.1 MPa, 0.2 MPa, 0.4 MPa and 0.8 MPa.

Residual volatile induced voids

The effect of residual volatile of laminates on void formation during resistance welding process was qualitatively studied. The generation of moisture induced voids was studied as an example. The polymer pressure, P_p, was calculated from the redistributed welding pressure in the composites, $P_{welding}$, assuming that the welding pressure is mainly results in internal stresses in the polymer and that the interaction between fabric and polymer can be ignored. To theoretically predict the influence of welding temperature and welding pressure on void nucleation and growth, the variables listed in Table 5 were used. Arbitrary values were used for R_0, S_0 and t, because, even though R_0, S_0 and t influence the void growth rate,[43,47] the trends will remain unchanged. Temperature dependent water vapour pressure was used.[27] As shown in Figure 7, either a higher welding temperature or a lower welding pressure was found to accelerate void formation, i.e. yielding a higher nucleation rate and faster void growth. Due to the non-uniform distributions of temperature and welding pressure inside the joints, un-even void nucleation and void growth were found inside the joints (see Figure 8). Higher void nucleation rates and faster void growths were obtained near the middle of the weld overlap than close to the edges, which were due to the higher welding temperature[28] and lower welding pressure towards the middle of the joints. Therefore, the areas in the middle parts of the joints and close to the welding interface were found to be the areas more prone to void formation.

Table 5. Constants used for the analysis of moisture induced void nucleation and growth

k_b (Boltzman)	γ (N/m)	$N\sqrt{2\gamma/\pi m}$	R_0 (mm)	S_0 (mm)	t (s)
1.38E-23	0.005 (1)	1.13E+25	0.0001 (2)	0.1 (2)	10 (2)

[1] A value taken from the range given in literature[33]

[2] Estimations

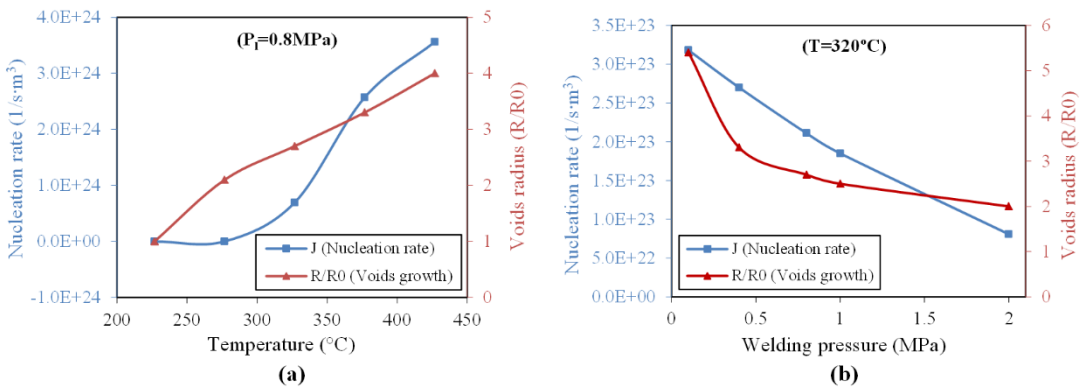

Figure 7. Effects of temperature (a) and welding pressure (b) on void nucleation and growth.

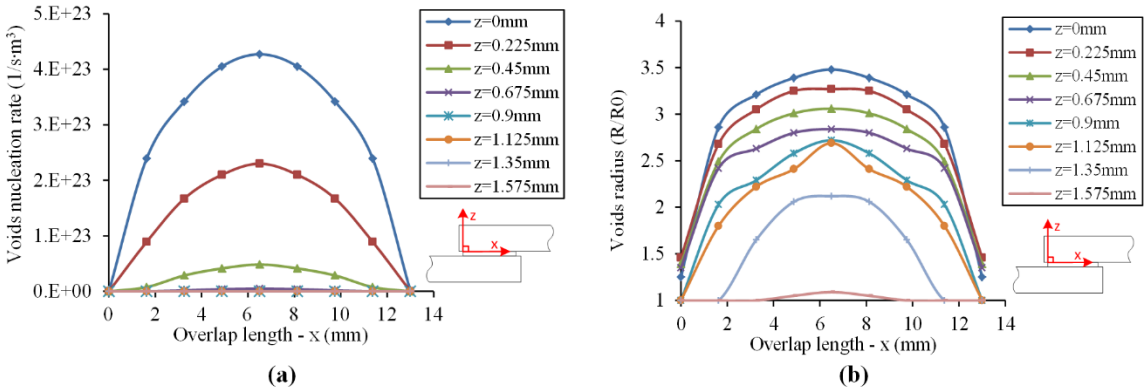

Figure 8. Distributions of void nucleation rate (a) and void growth (b) inside the joints for the maximum welding temperature, t = 55s.

Experiments were performed to investigate the effect of residual volatiles, namely moisture and NMP, on void generation in resistance welding of GF/PEI joints. The average weight content of residual moisture and NMP measured in the openly stored GF/PEI laminates (stored in an ambient environment with around 50% humidity) were around 1.1 wt% and 0.3 wt%, respectively. In order to investigate separately the effects of

NMP and moisture on the void formation in resistance welding, four different types of GF/PEI laminates were used and welded, as listed in Table 6. There was both residual moisture and NMP in Type-A laminates; only residual NMP in Type-B laminates; no residual volatile in Type-C laminates; and only residual moisture in Type-D laminates.

Table 6. GF/PEI laminates with different drying conditions

	Drying of prepreg at 260ºC	Laminate storage condition	Moisture content	NMP content
Type-A	No	Ambient enviroment (50% humidity) for 1 month	≈ 0.3 wt%	≈ 1.1 wt%
Type-B	No	Desiccator	0	≈ 1.1 wt%
Type-C	3 hours	Desiccator	0	0
Type-D	3 hours	2 weeks in water at room temperature	≈ 0.2 wt%	0

As shown in Figure9, almost no voids were observed in Type-B joints and Type-C joints, however, a considerable number of voids was found in Type-A and Type-D joints. It can be deduced that the residual moisture, other than the residual NMP, acts as the main cause of volatile induced voids in resistance welding. This should be related to the much higher vapour pressure seen for moisture with respect to NMP,[27] e.g. the vapour pressures of NMP and moisture at 320 °C are 0.08 MPa and 11.3 MPa, respectively. According to the classical nucleation theory, the pressure difference between the gas state and the liquid state of a volatile is vital for void nucleation. Therefore, nucleation of NMP was found to be more difficult than nucleation of moisture under a welding pressure of 0.8 MPa. Voids were found to preferentially concentrate in the middle area of the joints rather than at the edges, showing a reasonable agreement with the results of the theoretical

analysis. However, in contrast to the model prediction, the highest void density was not found near the welding interface, but inside the laminates. This might be explained by the migration of voids after formation, i.e. re-consolidation or void closure as proposed by Lu et al.[24]

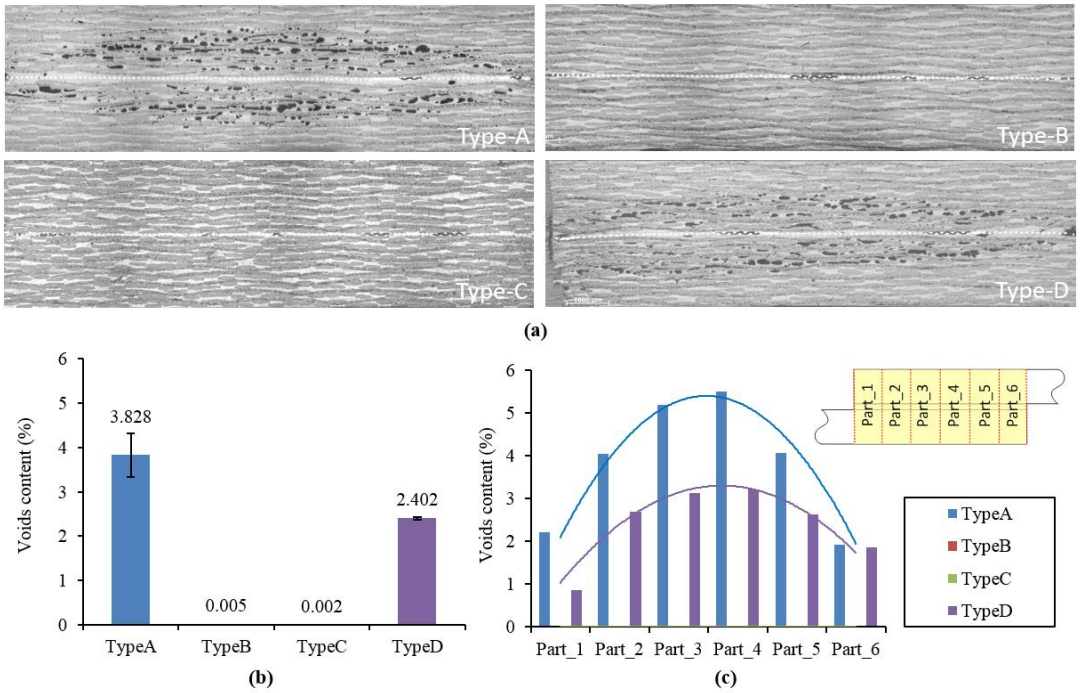

Figure 9. (a) Cross-section micrographs, (b) average void contents and (c) void distributions along the weld overlap of GF/PEI joints using laminates in different drying conditions: Type-A, Type-B, Type-C and Type-D.

As the residual moisture in the laminates was found to be crucial for void generation, experiments were performed to study whether drying the laminates prior to welding could be a practical way to remove the residual moisture for the ambient stored laminates, such as Type-A laminates. Before welding, Type-A

GF/PEI laminates were dried in an oven at 135 °C until a stable weight was reached. Compared to the joints welded with non-dried Type-A laminates (Figure 9), much less voids were found in the joints welded with dried Type-A laminates (Figure 10 (a)). However, unlike the Type-B laminates (Figure 10(b)), some voids were still found in the oven-dried Type-A laminates after welding, which could be due to the imperfection of moisture removing process. Moreover, micro-voids were widely observed in the dried laminates (Figure 10(a)), and they were probably not a consequence of welding but of the drying process.

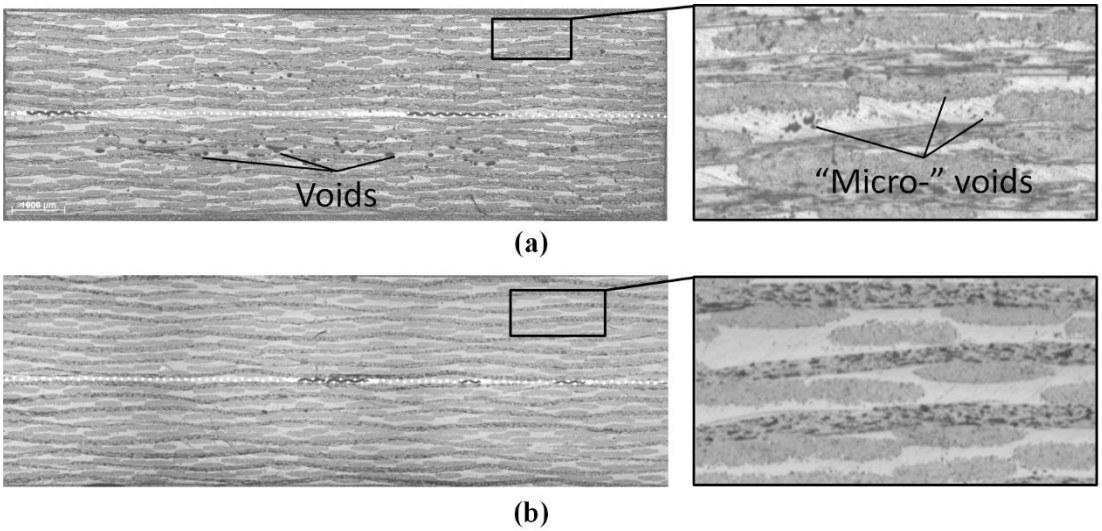

Figure 10. Cross-section micrographs of resistance welded joints using oven-dried Type-A GF/PEI laminates (a) and Type-B GF/PEI laminates (b).

The effect of welding pressure on the residual volatiles induced voids was also investigated. Type-A GF/PEI laminates, with both residual moisture and NMP in the laminates, were welded at different welding pressures of 0.8 MPa, 1.0 MPa, 1.2 MPa and 1.5 MPa. The void distributions and void contents inside the joints are shown in Figure 11, respectively. Void content was found to decrease with the welding pressure, in accordance with the model prediction. A welding pressure of 1.5 MPa was found to be sufficient to reduce the

voids content to a relatively low level of around 0.1%. Even though a higher pressure might help further reduce the void content, a too high welding pressure could lead to side effects, such as excess resin flow and vacuum cavities at the weld line, which might have a negative effect on the strength of the joints.[12]

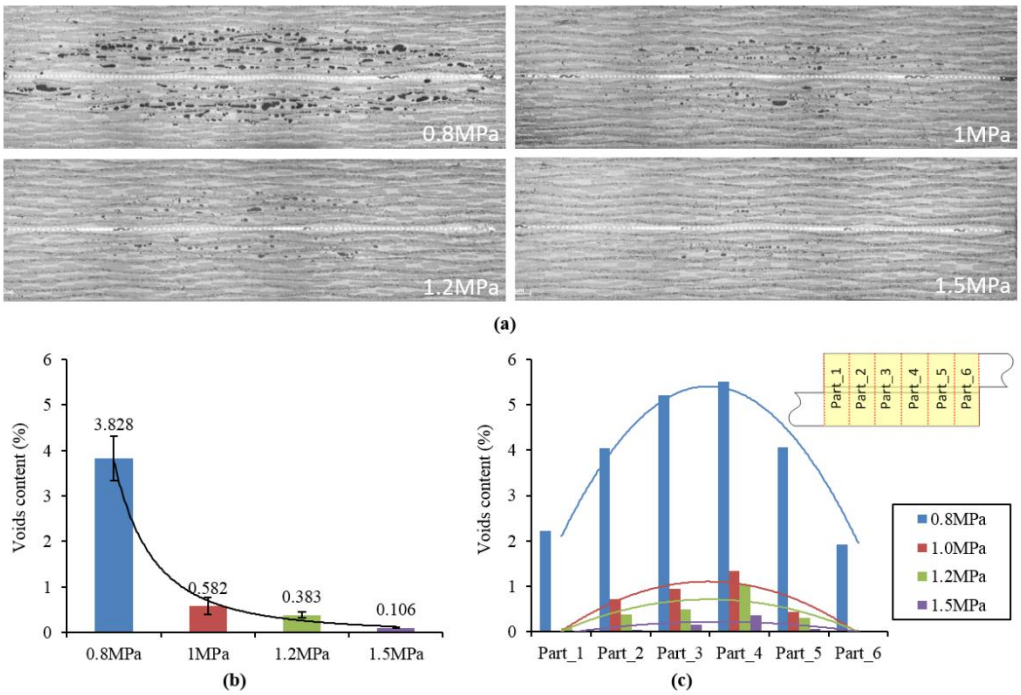

Figure 11. (a) Cross-section micrographs, (b) average void contents and (c) void distributions along the weld overlap of Type-A GF/PEI joints welded with different pressures of 0.8 MPa, 1 MPa, 1.2 MPa and 1.5 MPa.

Conclusion

The process induced voids during resistance welding of thermoplastic composites, in particular the residual volatile induced voids and fabric de-compaction induced voids in the adherends, were investigated. A combination of model and experimental analysis was performed to better understand the mechanisms

influencing void formation during the welding process. Resistance welding of glass fibre reinforced polyetherimide (GF/PEI) composites was performed using a metal mesh as the heating element.

Both residual volatiles and fibre de-compaction were found to induce voids during the resistance welding. Void formation was shown to be related to the welding pressure, welding temperature and the material properties of laminates, such as the matrix modulus and the fibre compressibility. Increasing welding pressure was found to help prevent the residual volatile induced voids and the fibre de-compaction induced voids. However, a higher welding pressure (1.5 MPa) was required to prevent residual volatile induced voids compared to fibre de-compaction induced voids (0.4 MPa). So, the voids induced by the residual volatiles were found to be more critical when welding under a moderate welding pressure, e.g. 0.8 MPa. The residual moisture in GF/PEI laminates was found to be the main cause of the volatile induced voids in resistance welding of GF/PEI rather than the residual solvent-NMP. Drying of laminates prior to welding was found to help reduce the void generation during welding, but the voids could not be completely prevented.

Due to the non-uniform distribution of temperature in the joints during welding, the compression stress in the middle part of the joints was found to be much smaller than at the nominal welding pressure, as a result of that more voids were generated in the middle of the joints than the edges. Future work should be focused on finding strategies to improve the uniformity of internal stress distribution in joints by reducing temperature gradients along the weld overlap, i.e. via tailoring/re-distributing welding energy at the weld overlap.

Acknowledgements

The authors would like to express their gratitude for the support provided by TenCate Advanced Composites, The Netherlands.

Funding

This research received no specific grant from any funding agency in the public, commercial, or not-for-profit sectors.

Reference

1. Eveno, E. C. and J. W. Gillespie (1988). "Resistance Welding of Graphite Polyetheretherketone Composites: An Experimental Investigation." Journal of Thermoplastic Composite Materials 1(4): 322-338.

2. Ageorges C, Ye L and Hou M. Advances in fusion bonding techniques for joining thermoplastic matrix composites: a review. Composites Part A: Applied Science and Manufacturing. 2001; 32: 839-57.

3. Yousefpour A, Hojjati M and Immarigeon J-P. Fusion Bonding/Welding of Thermoplastic Composites. Journal of Thermoplastic Composite Materials. 2004; 17: 303-41.

4. Stavrov D and Bersee HEN. Resistance welding of thermoplastic composites-an overview. Composites Part A: Applied Science and Manufacturing. 2005; 36: 39-54.

5. Ageorges C, Ye L and Hou M. Experimental investigation of the resistance welding of thermoplastic-matrix composites. Part II: optimum processing window and mechanical performance. Composites Science and Technology. 2000; 60: 1191-202.

6. Maffezzoli, A. M., J. M. Kenny, et al. (1989). "Welding of PEEK/carbon fiber composite laminates." SAMPE Journal 25(1): 35-40.

7. Wolfrath J, Michaud V and Manson JAE. Deconsolidation in glass mat thermoplastic composites: Analysis of the mechanisms. Composites Part a-Applied Science and Manufacturing. 2005; 36: 1608-16.

8. Xiao XR. A model for deconsolidation phenomenon in induction heating of thermoplastic resin composites. Ninth international conference on composite materials (ICCM9). Spain1993, p. 243-50.

9. M.D. W, P. B and E. MJ-A. Void evolution during stamp-forming of thermoplastic composites. 15th International Conference on Composite Materials (ICCM-15). Durban, South Africa2005.

10. Howie I, Gillespie JW and Smiley AJ. Resistance Welding of Graphite-Polyarylsulfone/Polysulfone Dual-Polymer Composites. Journal of Thermoplastic Composite Materials. 1993; 6: 205-25.

11. Stavrov D and Bersee HEN. Experimental investigation of resistance welding of thermoplastic composites with metal mesh heating element. SAMPE-Europe conference proceedings. Paris, France2004.

12. Dubé M, Hubert P, Gallet JN, Stavrov D, Bersee HE and Yousefpour A. Metal mesh heating element size effect in resistance welding of thermoplastic composites. Journal of Composite Materials. 2012; 46: 911-9.

13. Henninger F, Ye L and Friedrich K. Deconsolidation behaviour of glass fibre-polyamide 12 composite sheet material during post-processing. Plastics Rubber and Composites Processing and Applications. 1998; 27: 287-92.

14. Shi H, Villegas IF and Bersee HEN. Strength and failure modes in resistance welded thermoplastic composite joints: Effect of fibre–matrix adhesion and fibre orientation. Composites Part A: Applied Science and Manufacturing. 2013; 55: 1-10.

15. Michaud, V. and J.-A. E. Månson (2001). "Impregnation of Compressible Fiber Mats with a Thermoplastic Resin. Part I: Theory." Journal of Composite Materials 35(13): 1150-1173.

16. Michaud, V., R. Törnqvist, et al. (2001). "Impregnation of Compressible Fiber Mats with a Thermoplastic Resin. Part II: Experiments." Journal of Composite Materials 35(13): 1174-1200.

17. Ranganathan, S., S. G. Advani, et al. (1995). "Non-isothermal process model for consolidation and void reduction during in-situ tow placement of thermoplastic composites." Journal of Composite Materials 29(8): 1040-1062.

18. Pitchumani, R., S. Ranganathan, et al. (1996). "Analysis of transport phenomena governing interfacial bonding and void dynamics during thermoplastic tow-placement." International Journal of Heat and Mass Transfer 39(9): 1883-1897.

19. Gennaro, R., A. Greco, et al. (2010). "Numerical simulation of the microscale impregnation in commingled thermoplastic composite yarns." Advances in Polymer Technology 29(2): 122-130.

20. Lionetto, F., R. Dell'Anna, et al. (2015). "Ultrasonic assisted consolidation of commingled thermoplastic/glass fibers rovings." Frontiers in Materials 2.

21. Ageorges C and Ye L. Resistance welding of thermosetting composite/thermoplastic composite joints. Composites Part A: Applied Science and Manufacturing. 2001; 32: 1603-12.

22. Ageorges C, Ye L and Hou M. Experimental investigation of the resistance welding for thermoplastic-matrix composites. Part I: heating element and heat transfer. Composites Science and Technology. 2000; 60: 1027-39.

23. Ye L, Lu M and Mai Y-W. Thermal de-consolidation of thermoplastic matrix composites--I. Growth of voids. Composites Science and Technology. 2002; 62: 2121-30.

24. Lu M, Ye L and Mai Y-W. Thermal de-consolidation of thermoplastic matrix composites--II. "Migration" of voids and "re-consolidation". Composites Science and Technology. 2004; 64: 191-202.

25. Ageorges C and Ye L. Resistance Welding of Metal/Thermoplastic Composite Joints. Journal of Thermoplastic Composite Materials. 2001; 14: 449-75.

26. http://www.tencate.com. CETEX® PEI Technical Data. TenCate. 2009.

27. Saturated Vapor Pressure. http://ddbonline.ddbst.com/AntoineCalculation/AntoineCalculationCGI.exe ed.: DDBST GmbH, 2013.

28. Shi H, F.Villegas I and Bersee HEN. Modelling of Heat Transfer and Consolidation For Thermoplastic Composites Resistance Welding. 18th International Conference on Composites Materials. Jeju, South Korea2011.

29. Sabic. Thermal conductivity of Ultem 1000 PEI. http://www.sabic-ip.com/gepapp/eng/eddinter/eddchart; 2012.

30. Holmes ST and Gillespie JW. Thermal Analysis for Resistance Welding of Large-Scale Thermoplastic Composite Joints. Journal of Reinforced Plastics and Composites. 1993; 12: 723-36.

31. Predefined Built-In Materials for all COMSOL Modules. www.comsol.nl; 2012.

32. http://www.matweb.com/search/DataSheet. E-Glass Fiber, Generic. Matweb. 2012.

33. V. Vasiliev, E. Morozov. Advanced Mechanics of Composite Materials (Second Edition).

34. Kim YR, McCarthy SP and Fanucci JP. Compressibility and relaxation of fiber reinforcements during composite processing. Polymer Composites. 1991; 12: 13-9.

35. Robitaille F and Gauvin R. Compaction of textile reinforcements for composites manufacturing. I: Review of experimental results. Polymer Composites. 1998; 19: 198-216.

36. Saunders RA, Lekakou C and Bader MG. Compression in the processing of polymer composites 1. A mechanical and microstructural study for different glass fabrics and resins. Composites Science and Technology. 1999; 59: 983-93.

37. Ye L, Chen Z-R, Lu M and Hou M. De-consolidation and re-consolidation in CF/PPS thermoplastic matrix composites. Composites Part A: Applied Science and Manufacturing. 2005; 36: 915-22.

38. Pearce N and Summerscales J. The compressibility of a reinforcement fabric. Composites Manufacturing. 1995; 6: 15-21.

39. Saunders RA, Lekakou C and Bader MG. Compression in the processing of polymer composites 2. Modelling of the viscoelastic compression of resin-impregnated fibre networks. Composites Science and Technology. 1999; 59: 1483-94.

40. Colton JS and Suh NP. The nucleation of microcellular thermoplastic foam with additives: Part I: Theoretical considerations. Polymer Engineering & Science. 1987; 27: 485-92.

41. Han JH and Dae Han C. Bubble nucleation in polymeric liquids. II. theoretical considerations. Journal of Polymer Science Part B: Polymer Physics. 1990; 28: 743-61.

42. Blander M and Katz JL. Bubble nucleation in liquids. AIChE Journal. 1975; 21: 833-48.

43. Roychowdhury S, Jr. JWG and Advani SG. Volatile-induced Void formation in amorphous thermoplastic polymeric materials: I. Modeling and parametric studies. London, ROYAUME-UNI: Sage, 2001.

44. Arefmanesh A, Advani SG and Michaelides EE. An accurate numerical solution for mass diffusion-induced bubble growth in viscous liquids containing limited dissolved gas. International Journal of Heat and Mass Transfer. 1992; 35: 1711-22.

45. Ageorges C, Ye L, Mai Y-W and Hou M. Characteristics of resistance welding of lap shear coupons. Part I: Heat transfer. Composites Part A: Applied Science and Manufacturing. 1998; 29: 899-909.

46. Hexcel. Reinforcements Data Sheets. http://www.hexcel.com/Resources/Fabrics-Data-Sheets2012.

47. Leung SN, Park CB, Xu D, Li H and Fenton RG. Computer Simulation of Bubble-Growth Phenomena in Foaming. Industrial & Engineering Chemistry Research. 2006; 45: 7823-31.